Journal of Chromatography A, 1297 (2013) 204–212

Contents lists available at SciVerse ScienceDirect

Journal of Chromatography A

journal homepage: www.elsevier.com/locate/chroma

Column coupling isotachophoresis–capillary electrophoresis with mass spectrometric detection: Characterization and optimization of microfluidic interfaces

Pablo A. Kler[a], Tjorben N. Posch[a], Martin Pattky[a], Roald M. Tiggelaar[b,c], Carolin Huhn[a,*]

[a] Central Institute for Engineering, Electronics and Analytics, ZEA-3: Analytics, Forschungszentrum Jülich, Wilhelm-Johnen-Str., 52428 Jülich, Germany
[b] iX-factory GmbH, Konrad-Adenauer Allee 11, 44263 Dortmund, Germany
[c] Mesoscale Chemical Systems, MESA+Institute for Nanotechnology, University of Twente, P.O. Box 217, 7500 AE Enschede, The Netherlands

ARTICLE INFO

Article history:
Received 23 January 2013
Received in revised form 8 April 2013
Accepted 15 April 2013
Available online 3 May 2013

Keywords:
Two-dimensional electrophoretic separations
ITP–CE
Microfluidic interfaces
Mass spectrometry
Contactless capacitively coupled conductivity detection
Numerical modeling

ABSTRACT

Two-dimensional electrophoretic separations are one of the most promising tools for the continuously growing needs of different bioanalytical fields such as proteomics and metabolomics. In this work we present the design and the implementation of a two-dimensional electrophoretic separation coupled to mass spectrometry. We started our work studying the sample transfer characteristics of different microfluidic interfaces compatible with capillary coupling for two-dimensional electrophoretic separations. These junctions are aimed at method decoupling and sample transfer in a modular two-dimensional electrophoretic separation system. In order to perform the characterization of the interfaces, we carried out capillary electrophoresis experiments and numerical simulations using three cationic compounds under different flow conditions. The comparison of the experimental and simulation results enables us to clearly define the desirable characteristics of interfaces in order to achieve method orthogonality with lossless sample transfer in a two-dimensional separation system. Finally, we present a glass microfluidic chip as interface for the implementation of a novel hybrid modular system for performing two-dimensional electrophoretic separations involving isotachophoresis and capillary electrophoresis. In this setup we include mass spectrometric and contactless capacitively coupled conductivity detection to monitor the separation process. We demonstrate the ability of the setup to be used as a flexible analysis tool by performing preconcentration, separation, detection and identification of four different human angiotensin peptides.

© 2013 Elsevier B.V. All rights reserved.

1. Introduction

Two-dimensional electrophoretic separations consist of two independent separation steps arranged sequentially. Each step uses a different buffer composition and thus different separation mechanisms, which can be orthogonal under ideal conditions. These provide a selective relative displacement between analytes based on their different physicochemical properties [1]. The possible electrophoretic separations (dimensions) comprise a number of electromigrative separation techniques, such as capillary electrophoresis (CE), isoelectric focusing (IEF), isotachophoresis (ITP) and micellar electrokinetic chromatography, that have been widely used independently or coupled [2–4].

With the advent of microfluidic chips, a plethora of work has been conducted regarding sample preparation and separation, but also two- and multidimensional electrophoretic techniques have been demonstrated on chip [5]. Microfluidic chips are fluidic networks of channels with cross sectional dimensions in the micrometer range, with lengths in the range from millimeters to centimeters. They offer the possibility of defining highly complex fluidic patterns and the on-chip integration of sensors, electrodes and valves, thereby enabling very efficient implementations of two- and multidimensional electrophoretic separations. On-chip column coupling of electromigrative separation techniques involves microvalves for fluid flow decoupling between channels [6] or end-column flow suppressors [7]. Microfluidic chips, however, have the disadvantage that automated injection and standard detection techniques are currently not well established for routine analysis or rapid tests [8]. Particularly, the coupling of chip technology to mass spectrometry (MS) is at present not completely solved, even though some promising achievements were made [9–11].

In contrast, commercial equipment for classical capillary electrophoresis offers highly optimized and flexible instrumentation

* Corresponding author. Tel.: +49 2461 616873.
E-mail address: c.huhn@fz-juelich.de (C. Huhn).

0021-9673/$ – see front matter © 2013 Elsevier B.V. All rights reserved.
http://dx.doi.org/10.1016/j.chroma.2013.04.046

modules for automatic injection, pressure regimes and electric potential control, with robust coupling to optimized detection systems such as UV, MS, or contactless capacitively coupled conductivity detection (C^4D) [3].

Particularly ITP–ITP or ITP–CE implementations can be found in the literature using commercially available instrumentation [12,13]. The main drawback of these systems is the presence of semipermeable membranes and valves, controlling the hydrodynamic and electrical regimes of the system. Moreover, strong constraints exist regarding the dimensions of the columns for each separation. Several interfaces can be found in literature for the implementation of two-dimensional separations involving membranes [14], porous surfaces [15], polymer interfaces with considerable dead volume [16–18] or complicated dialysis loops [19], not completely suitable for efficient and flexible ITP–CE applications, especially in case of biomacromolecules with strong adsorption tendency. The interface proposed by Lee and coworkers [20,21] does not involve valves or complex fluidic elements, but has strong restrictions regarding the inner and outer diameter of the capillaries. Also, due to the fact that an open interface was used, it is not possible to completely transfer the sample from one column to another. Some of these 2D interfaces have also been implemented in systems with MS detection, using different customized (home-built) approaches such as, among others, the pumping of sample via sheath liquid [22] or a PTFE coupling device for transfer capillaries [23].

In order to obtain an efficient two-dimensional separation at least two aspects have to be ensured: (1) a high degree of orthogonality, which can be achieved by performing separation methods like ITP, IEF and CE in separated (decoupled) columns enabling different background electrolyte compositions with independent conditions for fluid flow and electric field [24]; and (2) a minimized loss (ideally zero) in the sample transfer process between steps. These conditions evoke the need to develop an efficient technique or configuration for decoupling and sample transfer between columns in order to avoid sample transport defects like band broadening, excessive tailing or even sample stacking at the interface [25].

In this manuscript we present our modular approach based on taking advantage of current and well developed commercially available technology, which is combined with suitable microfluidic interface designs for two-dimensional electrophoretic separations. Under this paradigm, the challenge consists in coupling the current capillary-oriented 1D CE technology with microfluidic elements, in order to produce two-dimensional electrophoretic separations provided with an efficient sample transfer mechanism and well established detection and identification methods.

At first, we perform the characterization of two different interfaces for capillary coupling. One interface consists of a polymeric (PEEK) T-junction that enables simple and fast coupling and decoupling of three capillaries, and the other is a glass microfluidic chip with a fluidic network that contains “in-plane” fluidic accesses that are particularly compatible with fused silica capillaries regarding cross sections and surface properties [26]. The characterization process is achieved via the numerical and experimental evaluation of these interfaces, comparing them with an ideal interface, i.e. a capillary without geometrical or material surface transitions (referred to as intact capillary). We developed an extended 1D numerical model that enables us to evaluate two-dimensional flow arrangements by keeping the computational cost to a minimum, i.e. the computational cost of the simulation of single capillaries. The comparison of experiments and simulations of different interfaces enables us to determine desirable characteristics and critical factors on designing these interfaces and their integration to the separation and detection systems for two-dimensional electrophoretic separations.

Secondly, we test the developed concepts in a novel hybrid capillary-microchip platform performing a two-dimensional electrophoretic separation: ITP–C^4D/CE–MS. This platform enables us to sequentially perform ITP for on-line pre-concentration and intermediate detection using C^4D, followed by a highly efficient CE separation coupled with MS detection for identification and quantification. It is also possible to perform matrix removal in the first dimension with simple rearrangement of the voltage regime applied. This original implementation offers clear advantages compared with other attempts present in the literature particularly regarding the sample transfer efficiency, robustness and flexibility: our concept uses a closed system without dead volume and with uniform surface properties avoiding complex fluidic components such as valves or membranes. It is able to work with a broad range of capillary dimensions, regarding their inner diameter, and offers a standard, robust and reliable integration with the detection systems enabling fast and reproducible analysis. We used four different human angiotensin peptides as model analytes for the application tests. Since these analytes were also used in similar previous works [23,27], we can show that effective separation and identification of these peptides at lower sample concentrations is possible using this novel concept.

2. Modeling and simulation

Numerical modeling of the interfaces for column coupling improves the understanding of the different physicochemical parameters that determine the efficiency of each interface on method decoupling and sample transfer for two-dimensional electrophoretic separations. Modeling is thus a tool that enables us to quickly and precisely evaluate interfaces under different operative conditions of flow, voltage regime or buffer composition. Our work here is based on a previously developed numerical scheme using the finite element method (FEM) [28–30]. This simulation tool allows to solve 1D, 2D and 3D problems involving different physicochemical fields such as fluid mechanics, mass transport, and electric potential, taking advantage of the high performance of parallel computing environments [31].

In the case of a single capillary and pure electroosmotic flow, due to the aspect ratio and the axial symmetry of phenomena, 1D simulation tools are suitable to model and reproduce CE separations [32]. In cases of mixed flow, or more complex channel geometries it is mandatory to solve at least the flow field in a 3D domain. Due to the computational costs, solving the electrophoretic transport problem for all species at each time step in a 3D domain is not suitable for our analysis entailing excessive time consumption. As a trade-off, we only solved the steady 3D fluid flow in the complete domain geometry. Afterwards, extracted data of the velocity field were used for solving a transient extended 1D model (1D*) for the electrophoretic transport. This simulation scheme enables us to have a suitable numerical modeling tool for performance evaluation of the interfaces in a reasonable time frame.

In what follows we describe the basics of these numerical models concerning this particular application. More general details about physicochemical hypotheses and mathematical formulation of the FEM model can be found in the cited bibliography [28–30].

2.1. Single capillary model

In a single capillary, the electrophoretic transport of sample and background electrolyte (BGE) components can be modeled by a linear superposition of the migrative, advective, and diffusive

transport mechanisms. In a non-stationary mode, the concentration of each j-type specie (c_j) is governed by:

$$\frac{\partial c_j}{\partial t} + \nabla \cdot (-z_{ej}\Omega_j \nabla\phi c_j + \mathbf{u}_{eo} c_j - D_j \nabla c_j) = 0, \quad (1)$$

where Ω_j and D_j represent the electrophoretic mobility and the diffusion coefficient for the specie j, respectively, ϕ represents the externally applied electric potential, and $\mathbf{u}_{eo}$ the electroosmotic fluid velocity. Special attention deserves z_{ej}, which represents the effective charge of the specie j, calculated through the degree of dissociation of the specie at the local pH values.

We computed the electric potential along the capillary ϕ, using the charge conservation equation, based on the hypothesis of global electroneutrality:

$$\nabla \cdot \left(-F\sum_{j=1}^{N} {z_{ej}}^2 \Omega_j c_j \nabla\phi - F\sum_{j=1}^{N} z_{ej} D_j \nabla c_j + F\sum_{j=1}^{N} z_{ej} c_j \mathbf{u}_{eo} \right) = 0, \quad (2)$$

where F is the Faraday constant, and N is the number of different species present in sample and BGE. In order to model the electroosmotic flow we used the Helmholtz–Smoluchowski equation for calculating the electroosmotic velocity:

$$\mathbf{u}_{eo} = \frac{\epsilon\zeta\nabla\phi}{\mu}, \quad (3)$$

where ϵ is the electric permittivity, and μ the dynamic viscosity of the fluid. Finally, ζ represents the electrokinetic potential, calculated by solving the following non-linear equation [33]:

$$\sqrt{8\epsilon RTI}\sinh\left(\frac{F\zeta}{2RT}\right) = \frac{-en_s}{1+10^{(pK_S-pH)}e^{-F\zeta/(RT)}}. \quad (4)$$

where R is the universal gas constant, T is the temperature, I is the ionic strength, and n_S the number of specific sites that solid walls expose toward the fluid able to release or bind H^+ ions, with a dissociation constant K_S. For fused silica capillaries these values are $n_s = 0.35 \times 10^{17}\ m^{-2}$ and $pK_S = 3.51$ [33].

2.2. Extended model

Although the previous simulation scheme is fully compatible with single capillary systems (inherently 1D), it is not suitable for representing more complex spatial arrangements such as T-junctions, microfluidic chips, or mixed flow conditions. In order to surmount these limitations we extended our 1D model, providing it with the capability of modeling the effects of radial velocities and fluxes. In order to determine this radial velocity and how the axial velocity is affected, we solved the 3D steady fluid flow problem for the interfaces. The discrete 3D mesh for fluid flow FEM calculation for one of the interfaces used in this work is shown in Fig. 1a. Implementation of this tetrahedral mesh is laborious as well as the solution of the fluid flow problem, but it has to be done only once for each interface.

In order to solve this fluid flow problem we used the steady Navier–Stokes equation:

$$\rho(\mathbf{u}\cdot\nabla\mathbf{u}) = \nabla\cdot(-p\mathbf{I} + \mu(\nabla\mathbf{u} + \nabla\mathbf{u}^T)), \quad (5)$$

$$\nabla\cdot\mathbf{u} = 0. \quad (6)$$

where ρ is the fluid density. As boundary conditions, we used the Helmholtz–Smoluchowski equation to calculate the tangential slip velocity at the walls, also we imposed an outlet pressure of 0 Pa.

After solving the fluid flow field in the 3D domain we extracted the axial (u_a) and radial (u_r) velocity components by performing an average over each cross section at each node on the matched axial linear mesh. The values obtained for these fields are shown in Fig. 1b. From this figure, we can infer that it is possible to define a zone where the distortions in the velocity are significant both for radial and axial velocities; we call this region δ. In this region δ, the main effects related to sample dispersion develop, such as the sample stacking/destacking due to variations in axial velocity, and the recirculation effect due to the increase of radial velocity. Finally, including these modified velocity fields, the extended 1D* transport equation is defined as:

$$\frac{\partial c_j}{\partial t} + \nabla \cdot (-z_{ej}\Omega_j \nabla\phi c_j + \mathbf{u}^* c_j - D_j \nabla c_j) = 0, \quad (7)$$

where the velocity vector $\mathbf{u}^*$ has two components, u_a^* and u_r^*, the axial and radial components, respectively, calculated for each FEM mesh node i as

$$u_a^* = \begin{cases} ||\mathbf{u}||, & \text{if } i \notin \delta \\ ||\mathbf{u}|| - \nu_a u_a, & \text{if } i \in \delta, \end{cases}$$
$$u_r^* = \begin{cases} 0, & \text{if } i \notin \delta \\ \nu_r u_r, & \text{if } i \in \delta. \end{cases} \quad (8)$$

These characteristic parameters represent the different sources of sample distortions that we can define for the interfaces: ν_a models the decrease of the axial velocity due to the cross sectional change as well as the decrease of the electroosmotic flow (EOF) performance due to the change of surface properties; and ν_r models the increase of radial velocity due to the cross sectional change. Under ideal conditions, i.e. a continuous, intact capillary, with neither cross sectional transitions nor surface changes, ν_a and ν_r values are 0.

3. Experimental

3.1. Instrumentation, reagents, and working solutions

All electrophoretic separations were performed using an Agilent 7100 CE system (Agilent Technologies, Waldbronn, Germany) providing pressure and voltage regimes, injection control, and vial handling. MS detection was achieved using an Agilent 6520 Q-TOF system (Agilent Technologies, Palo Alto, USA).

The CE was coupled to the MS via a coaxial sheath liquid interface from Agilent using an Agilent isocratic pump 1260 (Agilent Technologies, Waldbronn, Germany) for delivering sheath liquid (50:50 (v/v) mixture of water:isopropanol, containing 1% acetic acid) at a constant volume rate of 4 μL/min. The Q-TOF was operated in the low mass range (100–1700 m/z) using the extended dynamic range mode acquiring 2.73 spectra/s. The Fragmentor was set to +175 V, the skimmer was set to +65 V. Nebulizer pressure was set to 0.28 bar and the drying gas was delivered at rate of 4 L/min at a temperature of 300 °C.

C^4D detection was performed using a Csense One detection system (CalvaSens GmbH, Aalen, Germany) and voltage switching was performed by two high voltage relays HM12-1A69-300 (MEDER electronic AG, Singen, Germany) manually controlled by a home made device.

We used two different interfaces to perform coupling between fused silica capillaries: (1) the T-junction P-888 PEEK MicroTee (IDEX H&S GmbH, Wertheim, Germany), depicted in Fig. 2a; and (2) a customized glass microfluidic chip (iX-factory GmbH, Dortmund, Germany), shown in Fig. 2b. The T-shaped microfluidic network was made in Borofloat glass, the channels are 60 μm wide and 25 μm deep. Fig. 2c presents the details and dimensions of the channels and connection network in the microfluidic chip. The fabrication protocol of these glass chips is similar to the procedure described in [34].

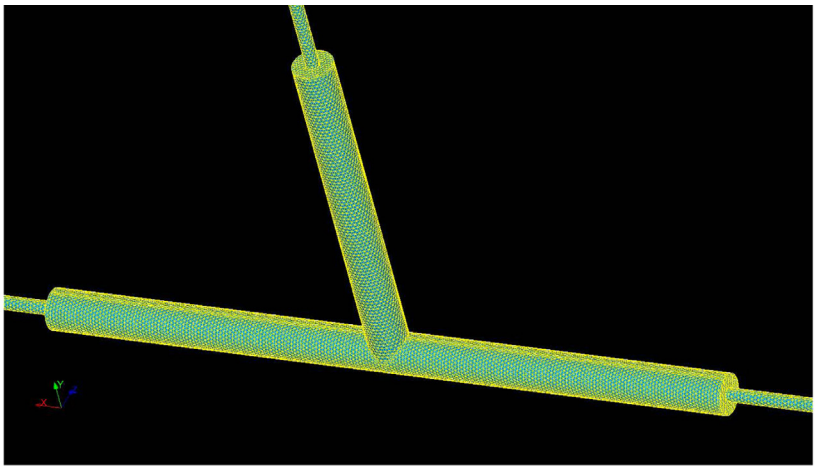

(a) Discrete mesh used in FEM calculations for the steady 3D fluid flow problem. Capillary column diameter is 50 μm.

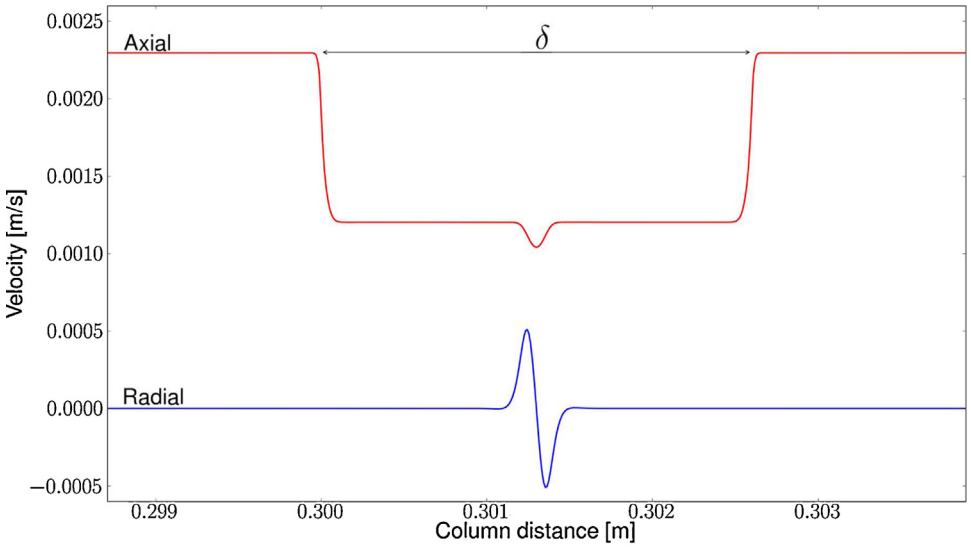

(b) Velocity profiles extracted from the 3D FEM solution.

Fig. 1. FEM mesh and obtained velocity profiles from the solution of the 3D steady fluid flow problem for one of the interfaces used in this work (T-junction P-888 PEEK MicroTee). (a) Discrete mesh used in FEM calculations for the steady 3D fluid flow problem. Capillary column diameter is 50 μm. (b) Velocity profiles extracted from the 3D FEM solution.

Ammonium hydroxide, isopropanol, histidine, and phenylalanine were bought from Fluka (Steinheim, Germany), and glacial acetic acid from Merck (Darmstadt, Germany). Norharmane and human angiotensins I, II, III, and IV were purchased from Sigma–Aldrich (Steinheim, Germany). LN coating solution (concentrate) was obtained from Target discovery (Palo Alto, CA, USA). All aqueous solutions were prepared with water from a Millipore Milli-Q purification system (Bedford, MA, USA). Fused silica capillaries (100 μm and 50 μm inner diameter (i.d.)) were purchased from Polymicro Technologies (Phoenix, AZ, USA). The epoxy glue used for capillary-to-chip coupling was Araldite Rapid (Huntsman Advanced Materials, Everberg, UK).

3.2. Characterization of interfaces: simulations and CE tests

In order to test the sample transfer performance of the PEEK T-junction and the glass microcfluidic chip, we performed CE separations of three cationic compounds: histidine, norharmane and phenylalanine. Sample transfer performance was evaluated in terms of peak shape distortion and migration time shifting. Experiments were performed first using a single capillary of 60 μm length and 50 μm i.d. Afterwards, the capillary was cut into halves. These halves, and a third capillary of the same length (30 cm, also 50 μm i.d.), were coupled using the two different interfaces. In the case of the PEEK T-junction, the coupling with the capillaries is straightforward using screw fittings, while for the glass chip, coupling was performed by gluing the capillaries into the chip accesses using an epoxy glue [34]. The free end of the third capillary was connected to a third vial, in a home-built vial holder, containing running buffer. Finally, all vial fluids were leveled in order to avoid hydrostatic pressure driven flows.

We chose the three different model analytes as follows: two substances with similar mobilities at the working pH (histidine and norharmane) in order to evaluate the different peak resolution of the systems, and one analyte with very low effective electrophoretic mobility at the working pH used to follow the electroosmotic or mixed flow (phenylalanine). Relevant physicochemical properties of analytes and buffer components, used for both simulation and experiments, are presented in Table 1. These properties were obtained from the *Simul 5* database (http://web.natur.cuni.cz/gas/). Due to the fact that we are working with diluted aqueous solutions we consider

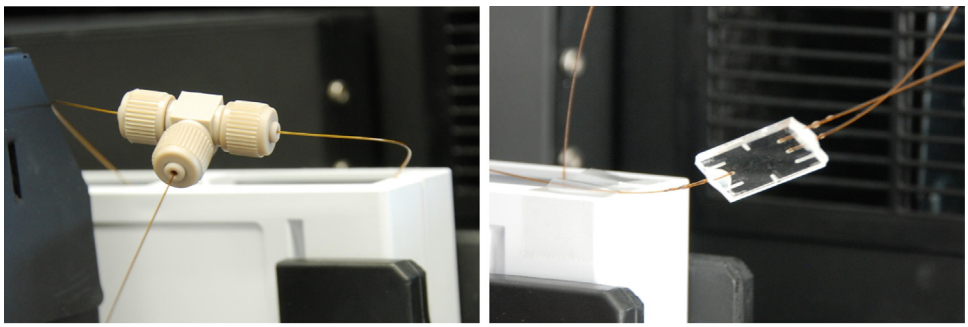

(a) PEEK T-junction. (b) Custom made glass microfluidic chip.

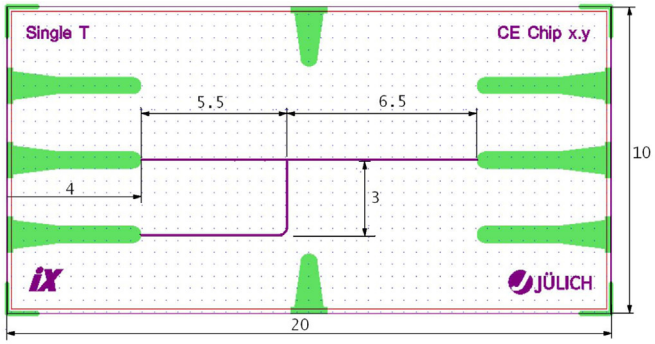

(c) Glass microfluidic chip layout, dimensions in mm. Adapted from sketch provided by manufacturer.

Fig. 2. Different interfaces characterized in this work including the microfluidic chip layout. Interfaces are shown with capillary connections and adaptation to the commercial capillary cartridge. The setups are mounted in the Agilent 7100 CE system. (a) PEEK T-junction. (b) Custom made glass microfluidic chip. (c) Glass microfluidic chip layout, dimensions in mm.

Adapted from sketch provided by manufacturer.

water properties for density, viscosity and electric permittivity. Simulations were performed on a desktop computer with single quad-core Intel i7 3770 3.4 GHz processor, QuickPath interconnect, 16 GB DDR3-1066 memory. Mesh calculations and preprocessing steps were performed using the Salome platform (http://www.salome-platform.org). Data postprocessing and visualization were done with Python Matplotlib [35] and Paraview (http://www.paraview.org).

Hydrodynamic and electrical parameters were: 5 s at 100 mbar for injection, and 8 min at +30 kV for separation; UV detection was performed using a wavelength of 214 nm, with an effective capillary length to the detection point of 51.5 cm. Running buffer was ammonium acetate 10 mM at pH 4.5, sample concentration was 10 μM. In order to obtain information on the performance of the sample transfer properties of the interfaces under different flow conditions, two experiments were performed: the first with normal EOF, and the second with a mixed flow including EOF and an external pressure of 50 mbar.

3.3. ITP–C^4D/CE–MS

Our numerical and experimental characterization of the interfaces enabled us to state that the glass microfluidic chip offers the best performance for two-dimensional electrophoretic separations. These results and conclusions are fully expanded in Sections 4.1 and 5. Moreover, in order to support our conclusions about this functionality, we implemented a two-dimensional electrophoretic separation consisting of ITP and CE, as first and second dimension respectively. We used two detection systems: C^4D for the intermediate detection for ITP, and MS as final detection and identification system after the CE step.

The classical CE instrument system was used in order to perform injection and flushing processes, applying electric potential and controlling the vial selection at the injection port. ITP separation was carried out in the capillary between the CE system and the microfluidic chip. This capillary was 20 cm long (100 μm i.d.) and guided through the C^4D detector, which was placed as close as possible to the chip. Due to the fact that the electrical isolation of the outlet port of the CE instrument is not intended to work at high voltage (HV), the second port of the chip was connected to a home made external auxiliary vial holder via a 40 cm long (50 μm i.d.) capillary. Finally, the third port of the chip was connected to the TOF-MS through a 30 cm long (50 μm i.d.) capillary. Prior to the experiments, coating of the inner surface of capillaries and glass chip was

Table 1
Physicochemical properties of BGE components and analytes.

Component	pK_a (+1)	pK_a (−1)	Mobility (10^{-8} m^2/V s)	Diffusivity (10^{-10} m^2/s)	Initial concentration
Ammonia	9.25	–	7.62	19.7	10 mM
Acetic acid	–	4.76	4.24	10.9	28 mM
Histidine	6.04	9.33	2.85	7.38	10 μM
Phenylalanine	2.13	9.26	2.70	7.11	10 μM
Norharmane	6.76	–	2.96	7.46	10 μM

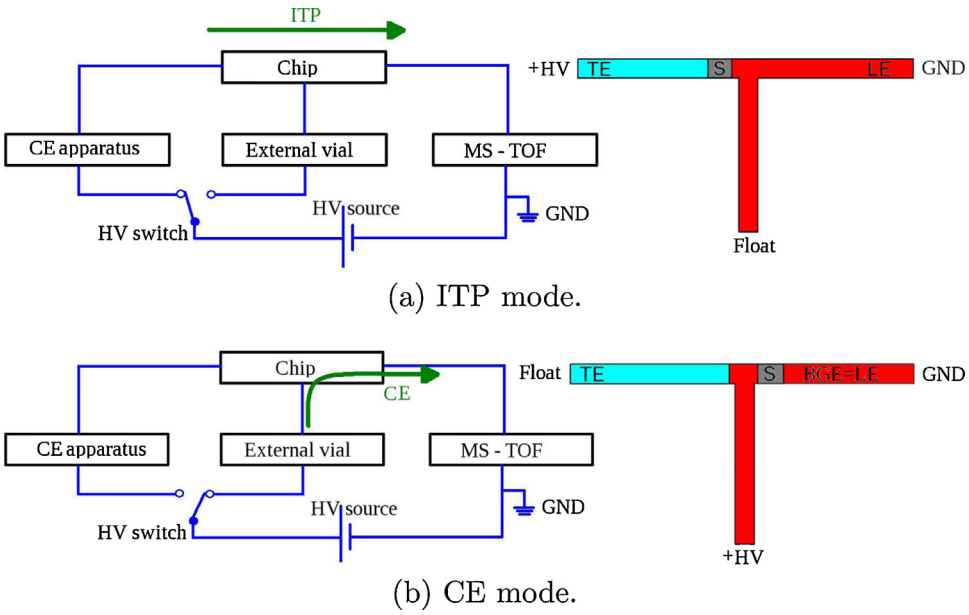

Fig. 3. Active electrical modes of operation for the ITP-C^4D/CE-MS setup. (a) ITP mode. (b) CE mode.

performed using LN coating following an overnight protocol [36].

The presented hybrid setup has three fundamental electrical modes of operation, which were used sequentially: floating mode, ITP mode, and CE mode. In the floating mode the HV switch is open, this mode was used to fill the complete fluidic circuit, consisting of the capillaries and the channels of the microfluidic chip, with leading electrolyte (LE) and for sample injection. Both processes were performed using the vials in the CE apparatus and the capillary connected to its inlet port. After injecting the sample plug, the terminating electrolyte (TE) vial was loaded to the inlet port of the CE and afterwards +14 kV were applied using the HV switch in the ITP mode (Fig. 3a). When the extrapolation of the C^4D output signal indicated that the TE-sample interface had arrived at the channel intersection inside the chip, the electric potential was switched to the auxiliary vial holder, and the system worked in the CE mode until the end of the measurement (Fig. 3b).

Initially we performed a 1D separation involving ITP–C^4D–MS with this setup. One of the drawbacks of this setup is that the C^4D detection is performed on-capillary (prior to the chip inlet), and not directly on-chip. Due to this, it is mandatory to establish the precise correlation between C^4D signal detection of the sample: TE boundary and the exact arrival time of this boundary at the channel intersection inside the chip. This correlation was obtained during the ITP–C^4D–MS experiment, using a combination of the C^4D signal and the recorded electric current in the CE instrument, which drastically changes when the ITP steps of different conductivities migrate through the channel intersection inside the chip. In our ITP–C^4D–MS and ITP–C^4D/CE–MS experiments we used ammonium acetate 10 mM at pH 4.5 as LE, and acetic acid 10 mM as TE. For the second step of ITP–C^4D/CE–MS separations, the BGE was also ammonium acetate 10 mM at pH 4.5. This means that we used the ITP–LE solution as BGE for the CE separation. In all cases, the injection procedure consisted in applying 50 mbar for 5 s. As model sample, human angiotensin I, II, III, and IV peptide mixture was used, at concentrations ranging from 1 nM to 10 μM.

4. Results and discussion

4.1. Interface characterization

For comparison, we initially performed experiments and simulations for the intact capillary in order to establish a reference performance with a system offering ideal characteristics of sample transfer. Results of the experiments and the simulations of the system for the intact capillary are shown in Fig. 4a for pure EOF and in Fig. 4b for mixed flow. From the high agreement of the experimental and simulated electropherograms shown in these figures, we can infer that the simulation scheme (i.e. equations, solving methods, and physicochemical constants) is suitable for predicting concentration fields for electrophoretic separations using the presented experimental setup.

Fig. 4c presents the results of the characterization of the PEEK T-junction showing the electropherograms obtained both numerically and experimentally for the separation under mixed flow conditions. By comparing Fig. 4b and c it is easy to infer that distortions on sample peaks for the commercial PEEK T-junction are incompatible with two-dimensional electrophoretic separations. From the comparison of our simulation results for the intact capillary ($\nu_a = 0$ and $\nu_r = 0$) and the PEEK T-junction ($\nu_a = 1.125$ and $\nu_r = 12.0$) we can state that distortions on sample distributions are generated due to: (1) change of the cross section (by approximately 200%), decreased axial velocity and increased radial velocity; (2) change of the surface properties (from fused silica to PEEK) affecting the EOF properties; and (3) decrease of the overall electric field efficiency, due to dispersion of the field lines. It is clear that sample distortions for analytes with low migration velocities (in this case, phenylalanine) are unacceptable.

In order to evaluate the impact of these effects, we performed simulations varying the parameters ν_a and ν_r (data not shown). From these results we can infer that the cross sectional change is the main reason for sample tailing. For example, when ν_r is set to 0, the tailing effect is negligible for any value of ν_a below 1.2. The only considerable effect is an increase of the detection time due to the decrease of the EOF and migration velocities due to the

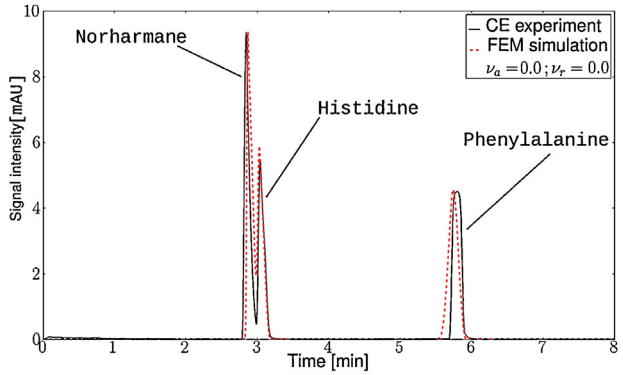

(a) Intact capillary, pure EOF.

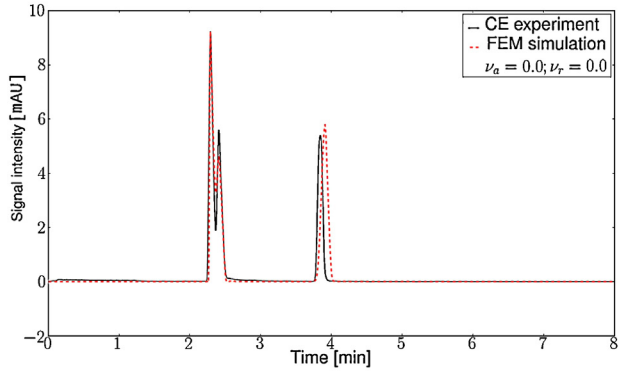

(b) Intact capillary, EOF + 50 mbar.

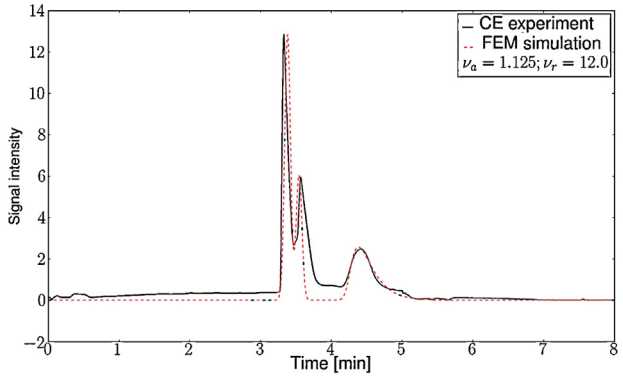

(c) PEEK T-junction, EOF + 50 mbar.

Fig. 4. Comparison between experimental results and FEM simulation under different flow conditions and for different setups. Hydrodynamic and electrical parameters were: 5 s at 100 mbar for injection, and 8 min at +30 kV for separation, UV detection was performed using a wavelength of 214 nm, with an effective capillary length of 51.5 cm. Running buffer was ammonium acetate 10 mM at pH 4.5. (a) Intact capillary, pure EOF. (b) Intact capillary, EOF + 50 mbar. (c) PEEK T-junction, EOF + 50 mbar.

change of the surface properties. From these numerical tests and experiments, it is clear that the sample transfer performance of the commercial PEEK T-junction is not suitable for two dimensional electrophoretic separations mainly due to the high dead volume. This dead volume generates important stacking/destacking as well as recirculation effects. Both effects can be observed in the simulation results via the velocity profiles shown in Fig. 1b, as well as in the experiments through the excessive tailing for phenylalanine shown in Figs. 4c and 5a, b.

Accordingly, the characteristics required for an efficient interface are: low dead volume or small cross sectional changes, and identical surface properties of capillaries and the interface. Glass

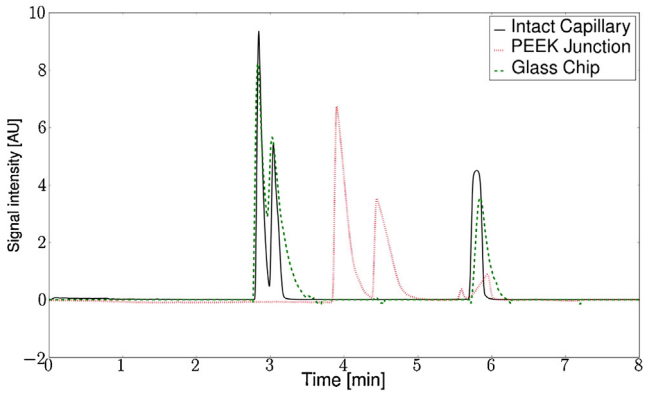

(a) Pure EOF.

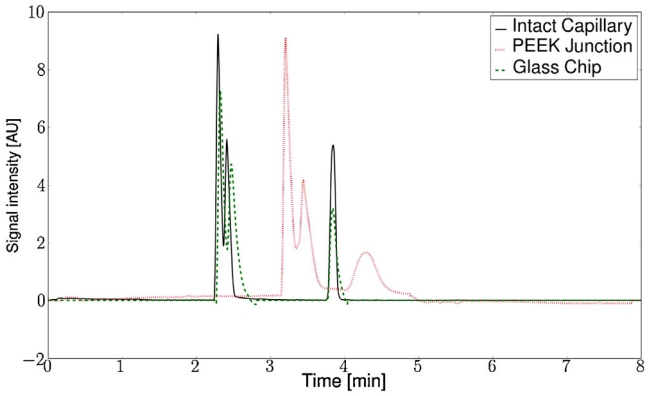

(b) EOF + 50 mbar.

Fig. 5. Comparison between signals from experiments using the three different setups. Experimental details are listed in Fig. 4. (a) Pure EOF. (b) EOF + 50 mbar.

microchip junctions, such as the one presented in Fig. 2b, meet these requirements. Fig. 5 presents the UV electropherograms obtained for the three different setups with the different conditions of flow. It can be observed that the migration times and separation efficiencies for the intact capillary and for the glass chip setup are similar. This means that distortions of electric field lines and the decrease of electroosmotic velocity due to surface heterogeneity are clearly overcome. There is still some tailing observed, which is due to the existence of a small dead volume mainly present in the region where capillaries are glued to the microchip. Nevertheless, the improvements in the signal peak shape corresponding to the slowest analyte (phenylalanine) are significant, compared to its same signal obtained for the PEEK interface.

4.2. ITP–C^4D/CE–MS

In order to demonstrate the real capabilities of the glass chip as interface for two-dimensional electrophoretic separations, we performed an ITP–C^4D/CE–MS analysis of a mixture of human angiotensins I,II,III, and IV. For all the experiments the setup and the experimental conditions described in Section 3.3 were used.

Initially we performed a 1D separation over the glass microfluidic chip interface involving ITP–C^4D–MS, using the setup in the single ITP mode (Fig. 3a). This experiment enables us to determine the correct timing for voltage switching in the ITP–C^4D/CE–MS experiments as explained in Section 3.3. Moreover, we also used this experiment in order to demonstrate that for these peptides, single ITP can provide a good preconcentration effect, but analyte resolution of the method is poor. These facts are illustrated in Fig. 6a and b showing C^4D and MS traces for a single ITP assay using a

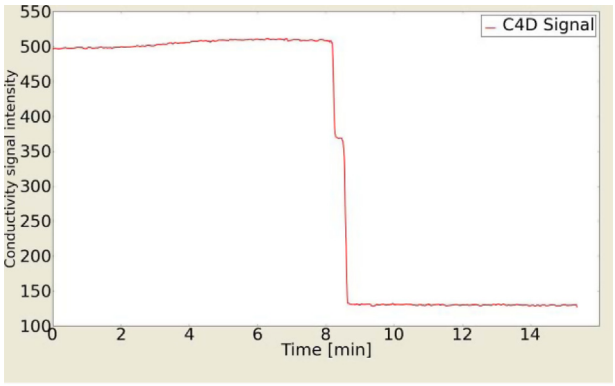

(a) C^4D signal recorded prior to the chip interface.

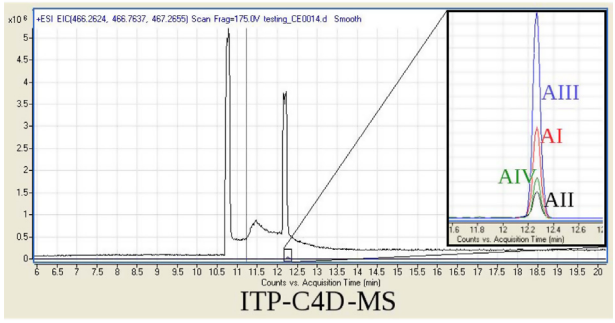

(b) MS signal.

Fig. 6. C^4D and MS signals for ITP of human angiotensin peptides using the ITP-C^4D-MS setup in the ITP mode shown in Fig. 3a. Hydrodynamic and electrical parameters were: 5 s at 50 mbar for injection, and 20 min at +14 kV for separation. LE was ammonium acetate 10 mM at pH 4.5, and TE acetic acid 10 mM. (a) C^4D signal recorded prior to the chip interface. (b) MS signal.

100 nM mixture of the four peptides as sample. Fig. 6a presents the C^4D signal acquired in front of the chip. Fig. 6b shows the MS signals for this analysis showing an accurate detection and identification of the four analytes, illustrating the preconcentration performance of the ITP step.

After ITP–C^4D–MS experiments and determination of the correct voltage switching time, we proceeded with the column-coupled ITP–C^4D/CE–MS analysis of the sample mixture at different sample concentrations. Fig. 7 presents the results for three different sample concentrations (1000 nM, 100 nM and 10 nM), showing the excellent preconcentration and separation efficiency of the proposed setup: the signals for angiotensin III (m/z = 466.0; charge = +2), angiotensin IV (m/z = 388.0; charge = +2), and angiotensin II (m/z = 523.6; charge = +2) maintain the correlation between signal magnitude and concentration, exhibiting higher peaks for higher concentrations. This correlation is not observed for angiotensin I (m/z = 648.3; charge = +2 and m/z = 432.7; charge = +3). Also, for the 10 nM sample a migration time shift for angiotensins II and IV can be observed. The reasons for these two atypical phenomena are not clear to us yet, but could be related to some lack of precision on the voltage switching time.

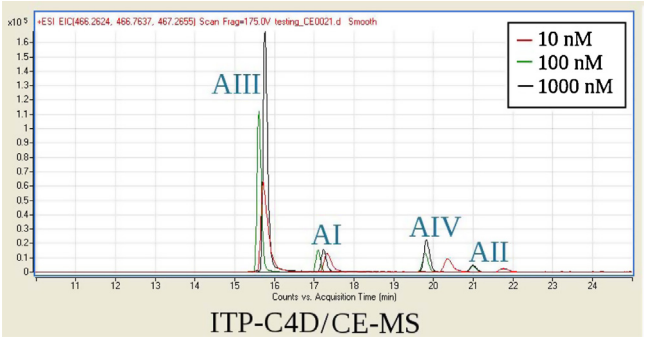

Fig. 7. MS signal for the ITP-C^4D/CE-MS analysis of different concentrations of human angiotensin peptides using sequentially the ITP and CE modes shown in Fig. 3a and b. For the CE separation ammonium acetate 10 mM at pH 4.5 was used as BGE, other experimental parameters are mentioned in Fig. 6.

5. Conclusions

We modeled and tested the performance of two different T-junctions in order to evaluate the sample transfer characteristics of these interfaces for two-dimensional electrophoretic separations. We developed and validated an extended 1D finite element model that enabled the quick and precise evaluation of these interfaces for electrophoretic separations under different physicochemical conditions.

Numerical modeling and experiments demonstrated that with a commercial PEEK T-junction electric and fluid flow fields are significantly distorted which causes unacceptable defects in sample transport. The deficiencies in sample transfer are enlarged for low mobility analytes, mainly due to the high dead volume. Consequently, this kind of junction would only be useful to perform separations involving highly charged analytes, prevailing the migration over the advection effect. Nevertheless, we can conclude that this kind of junction is not suitable for the implementation of high performance two-dimensional electrophoretic separations.

Characterization of the performance of a glass microchip interface clearly demonstrates that problems related to surface heterogeneity and cross section changes can be overcome yielding a sample transfer efficiency close to that of an intact capillary. We have demonstrated that such glass chip interface is a suitable element for capillary coupling in the development of two-dimensional electrophoretic separations in hybrid platforms.

We implemented a two-dimensional electrophoretic separation system involving ITP and CE as separation techniques, and C^4D and MS as detection methods. We have explored a novel paradigm of coupling two-dimensional electrophoretic separations with mass spectrometry, by using a modular hybrid approach between microfluidic chips and commercial equipment. This novel modular hybrid approach combines the advantages of commercial analytical equipment for controlling injection pressure and electric potential, in the case of CE, and the well known detection and identification capabilities of modern TOF-MS, using a well established sheath liquid interface, but also benefits from the precision and efficiency of microfluidic chips for sample handling and transfer between columns. This efficiency is based on the tight coupling between fused silica capillaries and the glass microfluidic chip enabling the system to work in a completely closed valveless fluidic circuit from sample injection to MS detection, thereby avoiding extra components such as membranes or complicated polymeric interfaces.

We have demonstrated the capabilities of our hybrid setup by the preconcentration, separation, detection and identification of model peptides, i.e. human angiotensins, over a broad range of concentrations. Due to the high efficiency of sample handling and transfer of this novel hybrid system, effective separation and identification were reached, at lower sample concentrations than previously reported [23,27]. Finally, we conclude that this two-dimensional setup represents an excellent option as a novel concept for a flexible analytical platform aimed at complex analytical and bioanalytical tasks.

Acknowledgements

We thank the Initiative and Networking Fund, Helmholtz Enterprise for financial support, Dietrich Kohlheyer at the Institute of

Bio- and Geosciences (IBG-1, Forschungszentrum Jülich), Daniel Lutz and Peter Zipfl at CalvaSens GmbH, and John W. Batts at IDEX Health & Science LLC for their valuable collaboration.

References

[1] O. Smithies, M. Poulik, Nature 177 (1956) 1033.
[2] J. Busnel, N. Lion, H. Girault, Anal. Chem. 79 (2007) 5949.
[3] J. Marák, A. Staňová, V. Vaváková, M. Hrenáková, D. Kaniansky, J. Chromatogr. A 1267 (2012) 252.
[4] S. Hu, D. Michels, M. Fazal, C. Ratisoontorn, M. Cunningham, N. Dovichi, Anal. Chem. 76 (2004) 4044.
[5] S. Tia, A. Herr, Lab. Chip 9 (2009) 2524.
[6] Y.-C. Wang, M.H. Choi, J. Han, Anal. Chem. 76 (2004) 4426.
[7] D. Kaniansky, M. Masár, J. Bielciková, F. Iványi, F. Eisenbeiss, B. Stanislawski, B. Grass, A. Neyer, M. Jöhnck, Anal. Chem. 72 (2000) 3596.
[8] J. Jokerst, J. Emory, C. Henry, Analyst 137 (2012) 24.
[9] M. Brivio, R. Oosterbroek, W. Verboom, A. van den Berg, D. Reinhoudt, Lab. Chip 5 (2005) 1111.
[10] S. Ohla, P. Schulze, S. Fritzsche, D. Belder, Anal. Bioanal. Chem. 399 (2011) 1853.
[11] A. Chambers, J. Ramsey, Anal. Chem. 84 (2012) 1446.
[12] A. Procházková, L. Křivánková, P. Boček, J. Chromatogr. A 838 (1999) 213.
[13] R. Bodor, M. Žúborová, E. Ölvecká, V. Madajová, M. Masár, D. Kaniansky, B. Stanislawski, J. Sep. Sci. 24 (2001) 802.
[14] H. Liu, C. Yang, Q. Yang, W. Zhang, Y. Zhang, J. Chromatogr. B 817 (2005) 119.
[15] H. Liu, L. Zhang, G. Zhu, W. Zhang, Y. Zhang, Anal. Chem. 76 (2004) 6506.
[16] A. Lemmo, J. Jorgenson, Anal. Chem. 65 (1993) 1576.
[17] T. Hooker, J. Jorgenson, Anal. Chem. 69 (1997) 4134.
[18] D. Michels, S. Hu, R. Schoenherr, M. Eggertson, N. Dovichi, Mol. Cell. Proteomics 1 (2002) 69.
[19] L. Sheng, J. Pawliszyn, Analyst 127 (2002) 1159.
[20] S. Chen, M. Lee, Anal. Chem. 72 (2000) 816.
[21] C. Bowerbank, M. Lee, J. Microcolumn Sep. 13 (2001) 361.
[22] R. Tomáš, M. Koval, F. Foret, J. Chromatogr. A 1217 (2010) 4144.
[23] Z. Peterson, C. Bowerbank, D. Collins, S. Graves, M. Lee, J. Chromatogr. A 992 (2003) 169.
[24] D. Kaniansky, M. Masár, M. Danková, R. Bodor, R. Rákocyová, M. Pilná, M. Jöhnck, B. Stanislawski, S. Kajan, J. Chromatogr. A 1051 (2004) 33.
[25] M.A. Fazal, V.R. Palmer, N.J. Dovichi, J. Chromatogr. A 1130 (2006) 182.
[26] R. Blanch-Ojea, R. Tiggelaar, J. Pallares, F. Grau, J. Gardeniers, Microfluid. Nanofluid. 12 (2012) 927.
[27] B. Zhang, F. Foret, B. Karger, Anal. Chem. 72 (2000) 1015.
[28] P. Kler, E. López, L. Dalcín, F. Guarnieri, M. Storti, Comput. Methods Appl. Mech. Eng. 198 (2009) 2360.
[29] P. Kler, C. Berli, F. Guarnieri, Microfluid. Nanofluid. 10 (2011) 187.
[30] P. Kler, L. Dalcin, R. Paz, T. Tezduyar, Comput. Mech. 51 (2013) 171.
[31] L. Dalcin, R. Paz, P. Kler, A. Cosimo, Adv. Water Resour. 34 (2011) 1124.
[32] V. Hruška, M. Riesová, B. Gaš, Electrophoresis 33 (2012) 923.
[33] C. Berli, M. Piaggio, J. Deiber, Electrophoresis 24 (2003) 1587.
[34] R. Tiggelaar, F. Benito-Lopez, D. Hermes, H. Rathgen, R. Egberink, F. Mugele, D. Reinhoudt, A. van den Berg, W. Verboom, H. Gardeniers, Chem. Eng. J. 131 (2007) 163.
[35] J.D. Hunter, Comput. Sci. Eng. 9 (2007) 90.
[36] M. Pattky, C. Huhn, Anal. Bioanal. Chem. 405 (2013) 225.